Designer benzodiazepines' activity on opioid receptors: a docking study

Authors:

Valeria Catalani[1], Michelle Botha[1], John Martin Corkery[1], Amira Guirguis[1,2], Alessandro Vento[3,4,5], Fabrizio Schifano[1]

Affiliations:

1. Psychopharmacology, Drug Misuse & Novel Psychoactive Substances Research Unit, School of Life & Medical Sciences, University of Hertfordshire, College Lane Campus, Hatfield, United Kingdom
2. Swansea University Medical School, The Grove, Swansea University, Singleton Park, Swansea, United Kingdom
3. Department of Mental Health, ASL Roma 2, Rome, Italy
4. Addictions' Observatory (ODDPSS), Rome, Italy
5. Guglielmo Marconi' University, Rome, Italy

Corresponding author

Valeria Catalani

v.catalani@herts.ac.uk

Contact emails:

m.botha@herts.ac.uk

j.corkery@herts.ac.uk

amira.guirguis@swansea.ac.uk

alessandrovento@gmail.com

f.schifano@herts.ac.uk

Running title: Designer Benzodiazepine activity on opioid receptors

ABSTRACT

Background. Previous studies have reported that benzodiazepines (BZDs) seem to enhance euphoric and reinforcing properties of opioids in opioid users so that a direct effect on opioid receptors has been postulated together with possible synergistic induction of severe side-effects due to their co-use. This is particularly worrisome given the appearance on the market of designer benzodiazepines (DBZDs), whose activity/toxicity profiles are scarcely known.

Objectives. This study aimed to evaluate, through computational studies, the binding affinity (or lack thereof) of 101 DBZDs identified online on the kappa, mu, and delta opioid receptors (K, M, DOR); and to assess whether their mechanism of action could include activity on t of the latter

Methods. MOE® was used for the computational studies. Pharmacophore mapping based on strong opioids agonist binder's 3D chemical features was used to filter the DBZDs. Resultant DBZDs were docked into the crystallised 3D active conformation of KOR (PDB6B73), DOR (PDB6PT3) and MOR (PDB5C1M). Co-crystallised ligands and four strong agonists were used as reference

compounds. A score (S, Kcal/mol) representative of the predicted binding affinity, and a description of ligand interactions were obtained from MOE® .

Results. The docking results, filtered for S < -8.0 and interaction with the aspartic acid residue, identified five DBZDS as putative OR binders across the three ORs: ciclotizolam, fluloprazolam, JQ1, Ro 48-6791, Ro 48-8684.

Conclusion. It may be inferred that at least some DBZDs may have the potential to activate opioid receptors. This could mediate/increase their anxiolytic, analgesic, and addiction potentials, as well as worsen the side-effects associated with opioid co-use.

Keywords: Designer Benzodiazepines; Docking; Pharmacophore Mapping; NPS*finder*®; Kappa-delta-mu opioid receptors; MOE®;

1 INTRODUCTION

Benzodiazepines (BZDs) are one of the most prescribed classes of drugs across the world [1,2].They were introduced onto the market in the early 1960s as anxiolytics, sedatives, hypnotics, anticonvulsants, and muscle relaxants [3]. Historically, they have been prescribed to heroin/opioid users to minimise withdrawal symptoms [3]. However, in recent years, this particular therapeutic indication has become controversial due to the reported increase of co-abuse disorders and addiction potential between the two classes of substances [4–8]. Indeed, opioid use disorders are associated with high-risk behaviours such as polysubstance use, including self-managed poly-consumption of benzodiazepines or psychotropic substances similarly active as benzodiazepine receptor agonists [9,10].

The most common reasons for the use of BDZs in poly-drug consumption are to enhance the feeling of "down" derived from opioids [11], with both chemical classes working as central nervous system depressants (CNS) [12]; and to self-medicate treating negative emotional states, psychiatric disorders and opioid withdrawal symptoms [1]. Previous studies have reported that BZDs seem to enhance euphoric, analgesic, and reinforcing properties of opioids in opioid users [10,13,14]. As a result, whilst BDZs' main mechanism of action is the allosteric modulation of the gamma-aminobutyric acid A receptor (GABA-AR), a direct effect on the kappa, mu and delta opioid receptors (KOR, MOR, DOR) has been postulated [13,14]. Opioid receptors (ORs) belong to the large superfamily of seven transmembrane (7TM) G protein-coupled receptors (GPCRs) [15]. Agonist activation of the ORs causes analgesia, sedation, euphoria, and decreased respiration in MOR [16–18]; antinociceptive, analgesic, aversive and psychotomimetic effects (hallucination and dissociation) in KOR [19,20]; and antinociceptive, anxiolytic and antidepressant effects in DOR. MOR, in particular, is considered responsible for triggering the brain reward system and initiating addictive behaviours [21–23].

Evidence shows that both midazolam and diazepam have a direct effect on the spinal antinociceptive opioid receptors (KOR and DOR) [24] with reinforcing properties. A reinforcing effect on ORs has been reported as well for the anxiolytic properties of the BDZs. Their anxiolytic effects may indeed be mediated through the modulation of the endogenous opioid system [25]. However, the exact mechanism of interaction and the possible subtypes of opioid receptors involved are still unclear [25]. It has been observed that the systemic administration of non-selective opioid antagonists (i.e., naloxone, picrotoxine, and β-funaltrexamine), in both animal and human models, can interfere with

the anxiety-reducing effects of BZDs [26,27]. Moreover, naltrexone, a preferential antagonist of MOR, has been observed to reduce the effects of diazepam on response latency in rats, suggesting that some of diazepam's effects could be caused by a mechanism sensitive to naltrexone [28,29]. A role for amygdalar opioid receptor sites (MOR and DOR) in the anxiolytic effects of benzodiazepines has been postulated [25].

Moreover, in the quest for safe and effective antinociceptive agents, derivatives of 1,4-benzodiazepine (e.g., tifluadom) have been identified as possessing a selective affinity for KOR [30,31].

Normally, BDZs display side-effects as induced primarily cognitive and psychomotor impairments, agitation, amnesia, confusion, depression, and dementia. Individuals who co-use BZDs with opioids in recreational settings, could be susceptible to additive effects with increased risks of sedation, synergistic induction of respiratory depression, coma, and death [6,7,32–34].

Recently, the documented co-use of BZDs and opioids and their synergistic side-effect profiles [7,33,34] have become increasingly worrisome, due mainly to the appearance on the market of novel synthetic opioids (NSOs) [35] and designer benzodiazepines (DBZDs) [36]. These new/novel molecules belong to the group of New Psychoactive Substances (NPSs) [37] and are mostly compounds with safety/toxicity profiles that are not fully understood. Indeed, limited knowledge is available on their pharmacodynamics and pharmacokinetics [38,39].

DBZDs, even if accounting for only less than 2% of the total number of known NPSs [5,8], have been reported worldwide in most NPS hospitalisations and fatalities (post-mortem) [40], and particularly so in polysubstance consumption scenarios [41–43]. As classical BZDs, they are usually ingested with other sedatives, primarily opioids, to potentiate their effects; promote 'come down' after stimulant use; or unintentionally, as counterfeits of prescription benzodiazepines [40].

Previous studies conducted by our research group with the use of a web crawler, NPS*finder*®, identified a total of 101 DBDZs [44]. This list includes a number of DBZDs identified online (the majority of which were retrieved from isomerdesign.com), higher than the number reported by the UNODC and EMCDDA [45,46]. Their putative activity on the γ-aminobutyric acid (GABA)-A receptor (GABA-AR) [44] was assessed with the use of computational models (i.e., QSAR, molecular docking and pharmacophore mapping). Computational models have been indicated as highly reliable methodologies to predict both the biological activity and binding affinity of unknown molecules towards a known receptor, and are well-established, successfully/extensively used tools, especially for drug development [47].

In light of the above, it is postulated that DBZDs could have a direct effect on the ORs receptors. This could complicate their already scarcely known pharmacodynamics and aggravate their safety/toxicity profiles. To date, the activity profile of DBDZs with ORs has not been assessed. Indeed, it is important to better understand the possible risks/harm associated with the use/abuse of DBZDs, assessing their mechanism of action and identifying the relative target receptor. While conducting preclinical studies with dozens or hundreds of molecules may constitute an extremely time-consuming and costly exercise, computational models could be used as fast and reliable preliminary assessment methodologies to investigate this mechanism of action.

This study aimed to computationally evaluate the binding affinity (or lack thereof) of the 101 DBZDs identified online towards KOR, MOR, and DOR, with the use of pharmacophore and docking studies, to assess if their mechanism of action could include activity on opioids' receptors.

2 METHODS

2.1 Identification of DBZDs

A crawling/navigating software (i.e., NPS*finder*®) was used to identify those NPSs being discussed and offered for sale on the surface web in the timeframe November 2017-February 2021. For the full methodology refer to Catalani et al. [44].

2.2 Identification of reference compounds

Reference compounds necessary for the pharmacophore filtering and for the docking studies of the 101 DBZDs identified, were obtained from the ChEMBL database [48]. Homo sapiens MOR, KOR, and DOR targets were searched for in the database and strong agonist binders for each of them were identified among the activity data available [49–51]. The EC_{50} (i.e., the concentration inducing half of the maximum effect, assessed as stimulation of [35S]GTPgammaS binding) was the activity type used. For each of the ORs, twenty potent (i.e., low value of EC_{50}) molecules (agonists) were identified and used (Supplementary material Table S1). These were identified across assays to minimise biases. A decision was taken to include twenty compounds to obtain a good variety among the chemical structures, without compromising the analysis time of the computational studies.

2.3 Computational models

The computational analysis was carried out with MOE® 2020.0901 software developed in Canada by the Chemical Computing Group ULC [52].

2.4 Pharmacophore filtering

For each OR, a pharmacophore map was retrieved from the twenty potent agonists identified in the ChEMBL database (Table S1). The purpose of this exercise was to define pharmacophore features common to high biological activity values. All these molecules, uploaded as SMILES into the MOE® database, were converted to MOE® molecules and underwent an energy minimisation and partial charge calculation with the molecular mechanic's force field Amber10:EHT, using the general energy minimisation function [53]. Conformations (i.e., 3D coordinates) were obtained with the "conformational search" application and a potential energy E (kcal/mol) was reported. The stochastic search was used as the output method. The lowest energy conformations were used for flexible alignment. A set of alignments was computed, and a final score (S, kcal/mol) returned. S quantifies the quality of the alignment in terms of internal strain (U score) and overlap of molecular features (F value). Lower values indicate better alignment. For the purposes of this study, the default settings were used. From the list of returned alignments, the ones showing the lowest S value were analysed and used to generate a pharmacophore query. The pharmacophore editor application was used in the consensus mode to assign pharmacophore annotation points (e.g., H-bond donor, H-bond acceptor, etc.) to the 3D conformations of the DBZDs flexibly aligned. The unified annotation scheme was used. The consensus mode returns, for each annotation point (i.e., pharmacophore feature), a percentage that indicates how common that particular feature is to the set of molecules analysed. Only the features showing values > 50% (to include the most common features) were taken into account for the final pharmacophore description. The final pharmacophore maps generated for each OR underwent a "validation step" as they were used to filter three databases of know MOR, KOR and DOR ligands (Table S2).

2.5 Molecular docking

Molecular docking (MD) evaluates the binding affinity between a ligand (DBDZ) and the receptors (KOR, MOR, and DOR) using a mathematical algorithm. To perform the molecular docking studies, 3D crystallised structures of the receptor with co-crystallised agonist ligands were used. The latter were searched for in the Protein Data Bank (PDB) [54]. Crystallised 3D structures for KOR, MOR,

and DOR were identified and refined according to the source organism and resolution (the resolution obtained in the 3D structure is measured in Angstrom (Å)). The chosen 3D structures were prepared with the Quick Prep application, which sets the protonation state of all residues and energy minimises the protein structure to avoid any steric clash.

The active site (i.e., binding pocket) of the 3D structures, identified by the presence of the co-crystallised ligands, was used as a superposition point for docking. Due to the presence of co-crystallised structures no further search for active site was performed on the receptors. The ligands atoms were used as the docking "site" in the General docking panel. No pharmacophore constraint was added due to the diversity between the co-crystallised ligands and the DBZDs under evaluation and to avoid forcing poses for the latter. (For full details see Figure S1.) If solvent molecules were present in the crystal structure, they were included in the docking process.

Reference compounds (i.e., selective and potent binders) for each of the receptors were docked to evaluate MOE® placement and scoring methods. Various conformations (energetically reasonable 3D atomic configurations) of the reference compounds were positioned into the binding pocket and the optimal interaction geometry (the conformation of the ligand that best interacts with the ligand pocket) and its associated energy (each conformation has an energy status associated resulting from the orientation of the molecule chemical bonds) determined. For each of these optimal interactions, a final score (S, Kcal/mol) was returned. The lower the S value was, the stronger the predicted binding affinity [52]. Once the placement and scoring method were chosen, they were used to dock the DBZDs matching the pharmacophore maps. Instead of repeating the docking process multiple times (usually 3 [55]), the number of poses generated in the placement was increased from the default values of 30 to 100 to account for system variability.

3 RESULTS

3.1 Identification of reference compounds

Homo sapiens MOR (CHEMBL233), KOR (CHEMBL237), and DOR (CHEMBL236) targets were identified together with a set of twenty potent agonists for each of the OR, selected from the ChEMBL Activity Database [49–51]. These compounds are reported in supplementary material (Table S1), identified by their ChEMBL ID, and include peptide and non-peptide ligands. A total of five compounds (including the co-crystallised ligand) for each OR were extrapolated from the literature according to their strong activity as agonist binders and used as reference molecules for docking studies (Table S3).

3.2 Pharmacophore filtering

For each of the twenty potent agonists selected from the ChEMBL database, ten conformations were generated. The ones showing the most favourable energetic state were further aligned. Three pharmacophore consensus queries for KOR, MOR, and DOR were generated from the alignment showing the lowest S values and manually analysed (Figures 1-3). The alignments are reported as pdb files in the supplementary material. The resulting pharmacophore maps were "validated" via the filtering of agonist ligands databases (validations sets) extrapolated from ChEMBL (76 ligands for each receptor, Table S2). KOR pharmacophore matched 69 of the ligands (91%) included in the validation set, MOR 62 ligands (81%) and DOR 36 ligands (47%). These data suggested how MOR and DOR were more comprehensive pharmacophore, matching compounds with higher values of biological activity, while KOR was more selective towards those with lower activity values, i.e., more potent. When these queries were used to filter the list of 101 DBDZs (TableS4) identified by the

NPS*finder*® activity on the surface web (isomerdesign.com [44,56]), the resulting hits were: 16 molecules for KOR, 23 molecules for DOR, and 21 molecules for MOR (Table S5).

3.3 Molecular docking

From the available structures in the PDB database, PDB5C1M for MOR [57,58], PDB6PT3 for DOR [59,60], and PDB6B73 [61,62] for KOR were chosen for docking studies. These crystallised structures, obtained by X-ray diffraction, all represent the opioid receptors in their active conformations, in complex with the agonist BU72, the small molecule agonist DPI-287, and the potent epoxymorphinan opioid agonist MP1104 respectively. These ligands were used as superposition targets for docking calculation sets and as reference for ligand interactions.

The opioids characteristic agonists interactions, as identified in literature, with aspartic acid (Asp128, 138, 147), methionine (Met132, 142, 151), and valine (Val281, 300) residues can be observed in Figures 4-6 [57,59,61].

The DBZDs obtained from the pharmacophore filtering were docked into their respective opioid receptors (PDB5C1M, PDB6PT3 and PDB6B73) together with the four reference compounds (i.e., strong agonist binders) and the co-crystallised ligand (BU72, DPI-287 and MP1104).

London dG and GBVI/WSA dG [52] were used as the scoring methods for the placement (alpha triangle and refinement (induced fit) of the docking process in the General Dock Panel application. For each molecule, the docking poses generated were analysed according to the energetic S values returned for each pose and the type of interaction suggested for the latter. The most common interactions identified between the DBZDs, and the binding pockets are presented in Table 2.

For the binding affinity a cut-off was chosen after evaluation of S values returned for the reference compounds and co-crystallised ligands (BU72 (S= -10.15), DPI-287 (S= -8.58) and MP1104 (S= -9.79) (Table 1). In particular DBZDs showing S<-8.00 (the lower the value, the stronger the binding), were considered as putative strong binders. For the interactions with the residues of the binding pockets, particular regard was given to the ionic and hydrogen-bond mediated interactions with the aspartic acid (Asp128,138,147) and to the hydrogen-bond mediated ones with methionine () residues [57,59,61]. Indeed, as reported in the literature, the ionic Asp interaction is an essential trait to infer the activity of an index molecule on the ORs [63,64]. A total of six molecules for KOR, five for DOR and four for MOR meeting both criteria were identified (Table 1).

Cinazepam, cyprazepam, ciclotizolam, fluloprazolam, Ro 48-6791, Ro 48-8684, JQ1 were found to display good binding affinity and the mandatory ionic interaction with the Asp residues. In particular, ciclotizolam, fluloprazolam, Ro 48-8684, JQ1 showed these characteristics consistently across the three receptor subtypes, showing however diverse binding affinity value for diverse ORs. The docking poses for these DBDZs are included as pdb files in supplementary material.

The 2D ligand interactions maps for the three top scoring DBZDs on each OR are reported in Figures 7-9. Detailed ligand interactions are reported in table S6. Fluloprazolam, Ro 48-8684 and Ro 48-6791 interact with Asp residue via the charged amine in their R group . For these molecules, none of the nitrogen atoms of the benzodiazepines structure seems to be involved in the ionic interaction. The ionic interaction of JQ1 and ciclotizolam instead, is mediated by the charged nitrogen atom in position 4 of the diazepine core. The same is observed for the other two DBZDs, cinazepam and cyprazepam. All the top scoring DBZDs are either triazolo or imidazole-benzodiazepines. This results in the presence of benzotriazole and benzimidazole moieties in the molecule scaffold, something that identifies with the structure of the synthetic opioids class nitazenes [65].

DISCUSSION

To the best of our knowledge, this study is the first to evaluate the possible binding affinity between DBZDs and the three opioid receptors, KOR, MOR, and DOR, giving an insight into their possible mechanism of action.

For each ORs, the best alignment obtained from twenty potent agonist binders for each of the ORs was used to design a pharmacophore map for the filtering of 101 DBZDS previously identified online. The resulting pharmacophores confirmed the importance and the recurring presence of two aromatic features and a more complex feature that includes, across all three receptor subtypes, a cation, a hydrogen bond prone group and an hydrophobic centre. This more complex feature identifies the important tertiary amine group, positively charged, that has been found mandatory activate the ORs family [66,67]. Consistent with previous studies, the interaction between the charged amine and the aspartic acid residue can be mediated either by a hydrogen bond or ionic interaction (salt bridge), the latter being stronger and important for the activation of the receptor [68].

The majority of interactions with active ORs are hydrophobic or aromatic in nature, with two conserved polar interactions as the exception [57].The pharmacophore maps presented in Figures 1-3 are in line with what have been reported in the literature [69–71].

Due to the similarity of the pharmacophores obtained for the ORs, the lists of the filtered DBZDs share similar entries (Table S2). In particular, the following molecules seem to match all three pharmacophore queries: ciclotizolam, fluloprazolam, JQ1 , Ro 48-8684 and Ro 48-6791. . It should be noted that these are either partial agonists towards the GABA-AR [72], characterised by fast pharmacokinetics (i.e., rapid onset and short half-life) [73], or "unknown" molecules, identified as DBZDs but lacking any further information on activity profile (e.g., fluloprazolam).

The pharmacophore filtered molecules were docked and further analysed according to two criteria: their value of predicted binding affinity (S) and their capability of engaging ionic/hydrogen bond interactions with the aspartic acid residue of the ORs binding pocket (Asp128, 138, 147). The lack of the latter constituted a reason for rejecting the molecule as a putative OR binder. The cut-off for the S value was set to -8.0 (Kcal/ mol). Despite the fact that this cut-off is one order of magnitude lower than some of the very potent agonists/strong binders reference compounds (e.g., Leu-enkephalin, carfentanyl, etc.), DBZDs with such S values could still show good binding affinity. The five DBZDs that met both criteria are discussed as possible binders: JQ1, fluloprazolam, ciclotizolam, Ro 48-8684, and Ro 48-6791.

JQ1 is a thienotriazolobenzodiazepine that does not act as an agonist at the GABA-AR. It is not currently used in human clinical trials due to its very short half-life [74].

Fluloprazolam seems to be an unknown DBZD, and only reference to a patent was retrieved in literature [75]. . Ciclotizolam is a very well-known low efficacy partial agonist of GABA-AR [76].

Ro 48-8684 and Ro 48-6791 are benzodiazepines developed by Hoffman-LaRoche in the 1990s [77] to achieve an improved replacement for midazolam. Unfortunately, they did not show advantages over the parent drug and were never developed as therapeutics [78].

Studies conducted with Ro 48-8684 and Ro 48-6791 [78–80] reported considerably shorter duration of action as well as faster recovery from the deep hypnotic effect. In particular, for Ro 48-8684 a reduced sensitivity was observed after repeated increasing dosage administration, due to undetermined factors [78].

These DBZDs show a short duration of action, in line with a partial agonist activity profile and the results predicted for their biological activity on GABA-AR [44]. Indeed, previous QSAR studies [44] predicted very low biological activity for Ro 48-8684, Ro 48-6791, JQ1, and fluloprazolam on the GABA-AR in line with their partial agonist activity profile. The only oddly predicted value was for ciclotizolam, indicating that the molecule may have a strong activity in contrast with it being a weak binder.

Analysing the S values obtained with the docking studies (Table 1), it can be noted that JQ1, Ro 48-8684 and fluloprazolam display higher binding affinity toward MOR, with values similar or greater than those obtained for carfentanyl and fentanyl (S= -9.95, -8.44) (Table S2). They all show interaction with Asp147 and Met151, while none of them interacts with His297 (Figure 7), as observed for BU72 (Figure 4). JQ1 and Ro 48-8684 display the hydrophobic bond with Val300 (Figure 7). This interaction has been observed, so far, in the binding of morphinan ligands only with the recruitment of a bigger hydrophobic surface including I296, W318, and I322 [57]. It is interesting to note that JQ1, the top scoring DBZDS, seems to interact with the Asp147 residue only, while Ro 48-8684 and fluloprazolam bind Met151 as well (Figure 7). The distance of the ionic bond (respectively, 3.20 (JQ1), 3.58 (fluloprazolam), and 3.35 (Ro 48-8684) Å) suggests a slightly stronger interaction than BU72 (3.53 Å) (Table S6).

The same very strong binding affinity is not observed for KOR, towards which the DBZDs display S values that are roughly one unit lower than the reference compounds and the epoxy morphinan MP1104 (Table1). It could be inferred that lower S values mean an activity threshold moved towards a greater order of magnitude when compared to MP1104. However, considering the latter has a picomolar KOR binding affinity [61], one can assume the higher concentration required to activate a response [55] will still fall in the lower nM range. Ro 48-8684 seems to be the most likely to bind KOR (S=- 8.74), followed by JQ1 and ciclotizolam. The distance of their ionic bond to Asp138, respectively, 3.91 and 3.02 and 3.3.35 Å, suggests a strength interaction similar to MP1104 (3.02 Å). The interactions for each molecule are presented in Figure 8, confirming the binding to Asp138.

A similar profile of binding affinity is observed for DOR. The DBDZs seem to show less affinity when compared to the reference compounds (Table 1), but the same affinity of the co-crystallised ligand DPI-287 (S= -8.58). Their interaction profile is presented in Figure 9.. Ro 48-8684 seems to be the molecule showing again the best affinity (S= -8.70). The distance of its ionic interaction (3.20) (Table S6)suggests it to be slightly weaker than DPI-287 (2.72), in line with the binding prediction (Figure 9). This applies as well to Ro 48-6791 (3.11) and fluloprazolam (3.61).

It is interesting to note that all the top scoring DBZDs, being either triazolo or imidazole-benzodiazepines, show structural similarity to midazolam, which was shown to have a direct effect on the spinal antinociceptive opioid receptors (KOR and DOR) [24]. For the scope of this paper a comparison with midazolam, together with other GABAergic currently used in the anaesthesia was carried out. A set of six commonly used GABAergic anaesthetic, including midazolam, diazepam and lorazepam [81] , was compiled (Table S7) and docked in the ORs. Only the anaesthetic possessing a nitrogen atom in their chemical formula were included. When docked in the ORs, midazolam was the only anaesthetic showing ionic interaction with Asp147 in MOR, with an S value of -7.33. The latter suggests a low binding affinity in line with the literature [13,14,24]. Same ionic interactions were observed for KOR and DOR.

No interaction with the aspartic acid residue was observed for the others anaesthetic, suggesting that anaesthetic/ analgesic action may be the result of interactions other than those with ORs. Moreover, these molecules showed S values higher than -7.0, hence almost two orders of magnitude lower than those observed for the DBZDs (TableS7).

Compared to midazolam (TableS7), the top scoring DBZDs seems to show higher binding affinity towards the ORs (Table1).

These results suggest how those obtained for the DBZDs, could be of value especially if one considers the presence of benzotriazole and benzimidazole moieties in the scaffold of these molecules, and their similarity with the nitazenes class of synthetic opioids.

Despite the docking results obtained for each molecule are only an educated guess, a prediction of the binding affinity towards ORs, they can still be considered of value due to the comparison with those obtained for well-known strong agonist binders and the respective ORs co-crystallised ligands [55]. This comparison, together with the identification of ionic interactions and the fact that docking score function has been proven capable of predicting crystallographic binding orientations [82,83], could support the thesis that these DBZDs may be able to acts on ORs, and not just fit in the binding pocket. However, to confirm or refute this hypothesis, further and more sophisticated computational methodologies (molecular dynamics), and/or experimental (i.e.. *in vitro* and *ex vivo) approaches* are needed.

Moreover binding affinity does not give information on the agonist or antagonist nature of the binding. Indeed docking per se does not provide a measure to discern between the two. Nevertheless, considering that the pharmacophores were built using agonist ligands, the likelihood of these DBZDs behaving as agonists could be inferred.

These results give an interesting insight into the possible interactions and mechanisms of action of these five DBZDs. They all seem to possess low activity on GABA-AR (fluloprazolam excluded), however, expressing some of the agonist features (analgesic, antidepressant and anxiolytic), accompanied by fast pharmacodynamics.

Indeed, the two Ro compounds have a reported profile of action that differs from common BZDs, characterised by a rapid onset and rapid recovery from the deep hypnotic effect together with the development of tolerance.

It could be inferred that the particular pharmacodynamics observed, especially the fast onset and recovery timing, could be due to the recruitment and activation of opioids' transmission. Indeed, it has been reported that the binding pockets of the ORs analysed here are largely exposed to the extracellular surface cavity and cause very fast dissociation half-lives of some extremely potent opioids (e.g., buprenorphine, carfentanyl, etorphine) [67,84].

Moreover, activation of the ORs produces effects similar to the activation of GABA-AR. In particular: activation of MOR results in sedation as well as tolerance and respiratory suppression, as seen for the α1 isoform of GABA-AR [85]; activation of DOR results in anxiolytic and antidepressant-like effects [86–88] as seen for the activation of the α2 isoform [89]. Activation of KOR instead produces analgesic, hallucinogenic, and dysphoric effects [61], which have not been observed with GABA-AR activation. Analgesic properties have previously been reported for BDZs; however it is important to underscore that this could be due to other mechanisms than interaction with ORs. Indeed, it has been reported that the reduced complaints of pain following BZDs consumption is just an indirect effect of their depressant activity [90]. Further studies will be conducted on evaluating possible pharmacophore match between opioid and BDZs, to address the possibility of a common drug scaffold.

Finally, if one considers that the most powerful analgesic and addictive properties of opioids are mediated by MOR, the results obtained from the docking studies could suggest a reinforcement of the addiction potential of these DBZDs.

4 Limitations

The major limitation of this study is the restricted size of the dataset (20 compounds for each receptor) used to develop the queries for the pharmacophore mapping/filtering exercise. Other limitations include the use of one receptor active conformation and co-crystallised ligand only, the lack of consensus docking; the lack of previous experimental data assessing the experimental binding affinity of DBZDs on ORs; and the lack of clear information on agonist /antagonist activity of the mentioned DBZDs despite the use of agonist binders for the creation of the pharmacophores.can be assumed. Further studies will include the evaluation of the binding pocket pharmacophore for each of the three ORs; *in vitro* assays to obtain experimental data on the EC50 or Ki as per Vandeputte et al. [65]; and *ex vivo* assays to get insight in their possible G protein (or β-arrestin) pathways activation as suggested by Inoue et al. [91].

CONCLUSIONS

While DBZDs represent only a small percentage of the NPSs identified worldwide [45,46], they are molecules of strong interest in polysubstance consumption settings. Indeed, they are increasingly being reported with other CNS depressants (e.g., opioids) to enhance and prolong the 'down' of the latter, or to deal with their withdrawal effect. Moreover, fatalities worldwide have been associated with their intravenous misuse [43]. The concomitant use of CNS depressants could lead to severe and worrisome synergistic enhancement of the adverse effects of both classes of substances, potentially resulting in life-threatening side-effects such as respiratory depression and coma.

This is particularly true for the combination of DBZDs and NSOs. Their pharmacodynamics and activity/toxicity profiles are largely unknown, and complications could arise if one considered a possible multitarget action profile for these new DBZDs.

It is, therefore, relevant to assess as much as possible their profile of activity, including possible actions on multiple receptors. This is particularly true for DBZDs because an interaction with opioids' transmission has already been postulated [13,14] and molecules containing the BZD scaffold synthesised in the quest for selective ORs ligands [30,31]. To achieve this, computational simulations, including, but not limited to docking and pharmacophore studies, could be used to elucidate the mechanism of action of these unknown molecules and help understand the possible threat (side-effects) associated with the latter. Computational studies can provide quick and reliable predictions of activity and affinity for a biological target, helping researchers to focus and direct their efforts and studies (e.g., in vitro, preclinical) towards a smaller number of NPSs.

Authors' contributions

VC and FS conceived the idea of the manuscript. All authors equally contributed to the initial planning of the data collection; VC undertook the data collection and drafted the paper itself. MB, AG, JC, and FS critically reviewed the final draft prior to submission, as well revisions resulting from peer-review. All authors have read and agreed to the published version of the manuscript.

ETHICS APPROVAL AND CONSENT TO PARTICIPATE

Not applicable.

HUMAN AND ANIMAL RIGHTS

No animals/humans were used for studies that are basis of this research.

CONSENT FOR PUBLICATION

Not applicable.

FUNDING

The authors declare that no funding has been received for this project.

AVAILABILITY OF DATA AND MATERIALS

The data supporting the findings of the article is available within the article.

CONFLICT OF INTEREST

The authors declare no conflict of interest, financial or otherwise.

ACKNOWLEDGMENTS

This article is part of VC's PhD research programme. The authors are grateful to Damicom srl, a small enterprise from Rome (Italy), whose professionals have developed the NPS*finder*® web-crawler and so generously have allowed here the testing of its potential.

SUPPLEMENTARY MATERIAL

Supplementary material is available on the publisher's website along with the published article.

REFERENCES

1. EMCDDA *Perspectives on drugs: the misuse of benzodiazepines among high-risk opioid users in Europe*; Lisbon, 2018;
2. EMCDDA *European Drug Report 2020: Trends and Developments*; Luxembourg, 2020;
3. EMCDDA Benzodiazepines drug profile Available online: http://www.emcdda.europa.eu/publications/drug-profiles/benzodiazepines_en (accessed on Apr 12, 2020).
4. De Wet, C.; Reed, L.; Glasper, A.; Moran, P.; Bearn, J.; Gossop, M. Benzodiazepine co-dependence exacerbates the opiate withdrawal syndrome. *Drug Alcohol Depend.* **2004**, *76*, 31–35, doi:10.1016/J.DRUGALCDEP.2004.04.002.
5. EMCDDA *European Drug Report 2021: Trends and Developments | www.emcdda.europa.eu*; Lisbon, 2021;
6. Liu, E.Y.; Tamblyn, R.; Filion, K.B.; Buckeridge, D.L. Concurrent prescriptions for opioids and benzodiazepines and risk of opioid overdose: protocol for a retrospective cohort study using linked administrative data. *BMJ Open* **2021**, *11*, 42299, doi:10.1136/bmjopen-2020-042299.
7. National Institute on Drug Abuse (NIDA) Benzodiazepines and Opioids Available online: https://www.drugabuse.gov/drug-topics/opioids/benzodiazepines-opioids (accessed on Nov

16, 2021).

8. UNODC *World Drug Report 2021*; Vienna, 2021;

9. Berro, L.F.; Rowlett, J.K. GABAA Receptor Subtypes and the Reinforcing Effects of Benzodiazepines in Remifentanil-Experienced Rhesus Monkeys. *Drug Alcohol Depend.* **2020**, *213*, 108076, doi:10.1016/J.DRUGALCDEP.2020.108076.

10. Poisnel, G.; Dhilly, M.; Le Boisselier, R.; Barre, L.; Debruyne, D. Comparison of five benzodiazepine-receptor agonists on buprenorphine- induced μ-opioid receptor regulation. *J. Pharmacol. Sci.* **2009**, *110*, 36–46, doi:10.1254/JPHS.08249FP.

11. Navaratnam, V.; Foong, K. Opiate dependence–the role of benzodiazepines. *http://dx.doi.org/10.1185/03007999009112688* **2008**, *11*, 620–630, doi:10.1185/03007999009112688.

12. Moore, J.J.; Saadabadi, A. Selegiline. *StatPearls* **2020**.

13. Goodchild, C.; Serrao, J. Intrathecal midazolam in the rat: evidence for spinally-mediated analgesia. *Br. J. Anaesth.* **1987**, *59*, 1563–1570, doi:10.1093/BJA/59.12.1563.

14. Rattan, A.; McDonald, J.; Tejwani, G. Differential effects of intrathecal midazolam on morphine-induced antinociception in the rat: role of spinal opioid receptors. *Anesth. Analg.* **1991**, *73*, 124–131, doi:10.1213/00000539-199108000-00004.

15. Waldhoer, M.; Bartlett, S.E.; Whistler, J.L. Opioid Receptors. *http://dx.doi.org/10.1146/annurev.biochem.73.011303.073940* **2004**, *73*, 953–990, doi:10.1146/ANNUREV.BIOCHEM.73.011303.073940.

16. Algera, M.H.; Kamp, J.; van der Schrier, R.; van Velzen, M.; Niesters, M.; Aarts, L.; Dahan, A.; Olofsen, E. Opioid-induced respiratory depression in humans: a review of pharmacokinetic–pharmacodynamic modelling of reversal. *Br. J. Anaesth.* **2019**, *122*, e168–e179, doi:10.1016/J.BJA.2018.12.023.

17. Ehrlich, A.T.; Kieffer, B.L.; Darcq, E. Current strategies toward safer mu opioid receptor drugs for pain management. *https://doi.org/10.1080/14728222.2019.1586882* **2019**, doi:10.1080/14728222.2019.1586882.

18. Severino, A.; Chen, W.; Hakimian, J.K.; Kieffer, B.L.; Gaveriaux-Ruff, C.; Walwyn, W.; Marvizon, J.C. Mu-opioid receptors in nociceptive afferents produce a sustained suppression of hyperalgesia in chronic pain. *Pain* **2018**, *159*, 1607, doi:10.1097/J.PAIN.0000000000001247.

19. Beck, T.C.; Hapstack, M.A.; Beck, K.R.; Dix, T.A. Therapeutic Potential of Kappa Opioid Agonists. *Pharmaceuticals* **2019**, *12*, doi:10.3390/PH12020095.

20. Paton, K.; Atigari, D.; Kaska, S.; Prisinzano, T.E.; Kivell, B.M. Strategies for developing kappa opioid receptor agonists for the treatment of pain with fewer side-effects. *J. Pharmacol. Exp. Ther.* **2020**, *375*, 332–348, doi:10.1124/JPET.120.000134.

21. Butelman, E.R.; Picetti, R.; Reed, B.; Yuferov, V.; Kreek, M.J. Addictions. In *Neurobiology of Brain Disorders: Biological Basis of Neurological and Psychiatric Disorders*; Academic Press, 2015; pp. 570–584.

22. Contet, C.; Kieffer, B.; Befort, K. Mu opioid receptor: a gateway to drug addiction. *Curr. Opin. Neurobiol.* **2004**, *14*, 370–378, doi:10.1016/J.CONB.2004.05.005.

23. Merrer, J. LE; Becker, J.A.J.; Befort, K.; Kieffer, B.L. Reward Processing by the Opioid System in the Brain. *Physiol. Rev.* **2009**, *89*, 1379, doi:10.1152/PHYSREV.00005.2009.

24. Cox, R.F.; Collins, M.A. The effects of benzodiazepines on human opioid receptor binding

and function. *Anesth. Analg.* **2001**, *93*, 354–358, doi:10.1213/00000539-200108000-00024.

25. Primeaux, S.D.; Wilson, S.P.; McDonald, A.J.; Mascagni, F.; Wilson, M.A. The role of delta opioid receptors in the anxiolytic actions of benzodiazepines. *Pharmacol. Biochem. Behav.* **2006**, *85*, 545, doi:10.1016/J.PBB.2006.09.025.
26. Billingsley, M.; Kubena, R. The effects of naloxone and picrotoxin on the sedative and anticonflict effects of benzodiazepines. *Life Sci.* **1978**, *22*, 897–906, doi:10.1016/0024-3205(78)90614-8.
27. Tsuda, M.; Suzuki, T.; Misawa, M.; Nagase, H. Involvement of the opioid system in the anxiolytic effect of diazepam in mice. *Eur. J. Pharmacol.* **1996**, *307*, 7–14, doi:10.1016/0014-2999(96)00219-1.
28. Richardson, D.K.; Reynolds, S.M.; Cooper, S.J.; Berridge, K.C. Opioid agonists and benzodiazepine agonists each increase food intake. Both also increase hedonic "liking" reactions to sweet tastes in rats. Do opioids and benzodiazepines share overlapping mechanisms of hedonic impact? *Pharmacol. Biochem. Behav.* **2005**, *81*, 657–663, doi:10.1016/J.PBB.2005.05.006.
29. Herling, S. Naltrexone blocks the response-latency increasing effects but not the discriminative effects of diazepam in rats. *Eur. J. Pharmacol.* **1983**, *88*, 121–124, doi:10.1016/0014-2999(83)90400-4.
30. Cappelli, A.; Anzini, M.; Vomero, S.; Menziani, M.; De Benedetti, M.; Sbacchi, P.; Clarke, G.; Mennuni, L. Synthesis, biological evaluation, and quantitative receptor docking simulations of 2-[(acylamino)ethyl]-1,4-benzodiazepines as novel tifluadom-like ligands with high affinity and selectivity for kappa-opioid receptors. *J. Med. Chem.* **1996**, *39*, 860–872, doi:10.1021/JM950423P.
31. Anzini, L.; Canullo, M.; Braile, C.; Cappelli, A.; Gallelli, A.; Vomero, S.; Menziani, M.; De Benedetti, P.; Rizzo, M.; Collina, S.; et al. Synthesis, biological evaluation, and receptor docking simulations of 2-[(acylamino)ethyl]-1,4-benzodiazepines as kappa-opioid receptor agonists endowed with antinociceptive and antiamnesic activity. *J. Med. Chem.* **2003**, *46*, 3853–3864, doi:10.1021/JM0307640.
32. Afzal, A.; Kiyatkin, E. Interactions of benzodiazepines with heroin: Respiratory depression, temperature effects, and behavior. *Neuropharmacology* **2019**, *158*, doi:10.1016/J.NEUROPHARM.2019.107677.
33. Boon, M.; van Dorp, E.; Broens, S.; Overdyk, F. Combining opioids and benzodiazepines: effects on mortality and severe adverse respiratory events. *Ann. Palliat. Med.* **2020**, *9*, 54257–54557, doi:10.21037/APM.2019.12.09.
34. Medicines and Healthcare products Regulatory Agency Benzodiazepines and opioids: reminder of risk of potentially fatal respiratory depression. Available online: https://www.gov.uk/drug-safety-update/benzodiazepines-and-opioids-reminder-of-risk-of-potentially-fatal-respiratory-depression (accessed on Oct 11, 2021).
35. Arillotta, D.; Schifano, F.; Napoletano, F.; Zangani, C.; Gilgar, L.; Guirguis, A.; Corkery, J.M.; Aguglia, E.; Vento, A. Novel Opioids: Systematic Web Crawling Within the e-Psychonauts' Scenario. *Front. Neurosci.* **2020**, *14*, 149, doi:10.3389/fnins.2020.00149.
36. Catalani, V.; Botha, M.; Corkery, J.M.; Guirguis, A.; Vento, A.; Schifano, F. Cognitive enhancers: computational models on benzodiazepines and racetams identified online. **2021**.
37. Schifano, F. Recent changes in drug abuse scenarios: The new/novel psychoactive substances (NPS) phenomenon. *Brain Sci.* 2018, *8*.

38. Lovrecic, B.; Lovrecic, M.; Gabrovec, B.; Carli, M.; Pacini, M.; Maremmani, A.G.I.; Maremmani, I. Non-medical use of novel synthetic opioids: A new challenge to public health. *Int. J. Environ. Res. Public Health* 2019, *16*.

39. Orsolini, L.; Corkery, J.M.; Chiappini, S.; Guirguis, A.; Vento, A.; De Berardis, D.; Papanti, D.; Schifano, F. "New/Designer Benzodiazepines": an analysis of the literature and psychonauts' trip reports. *Curr. Neuropharmacol.* **2020**, *18(9)*, 809–837, doi:10.2174/1570159X18666200110121333.

40. ACMD *Novel Benzodiazepines A review of the evidence of use and harms of Novel Benzodiazepines*; London, 2020;

41. Carpenter, J.E.; Murray, B.P.; Dunkley, C.; Kazzi, Z.N.; Gittinger, M.H. Designer benzodiazepines: a report of exposures recorded in the National Poison Data System, 2014–2017. *Clin. Toxicol.* **2019**, *57*, 282–286, doi:10.1080/15563650.2018.1510502.

42. UNODC *Non-medical use of benzodiazepines : a growing threat to public health ?*; Vienna, 2017; Vol. 18;.

43. UNODC *Current NPS Threats Volume III*; Vienna, 2020;

44. Catalani, V.; Botha, M.; Corkery, J.M.; Guirguis, A.; Vento, A.; Scherbaum, N.; Schifano, F. The psychonauts' benzodiazepines; quantitative structure-activity relationship (QSAR) analysis and docking prediction of their biological activity. *Pharm. 2021, Vol. 14, Page 720* **2021**, *14*, 720, doi:10.3390/PH14080720.

45. EDND EDND - Login page Available online: https://ednd2.emcdda.europa.eu/ednd/login (accessed on Nov 18, 2019).

46. UNODC Early Warning Advisory (EWA) on New Psychoactive Substances (NPS) Available online: https://www.unodc.org/LSS/Home/NPS (accessed on Feb 4, 2021).

47. Valerio, L.G.; Choudhuri, S. Chemoinformatics and chemical genomics: potential utility of in silico methods. *J. Appl. Toxicol.* **2012**, *32*, 880–889, doi:10.1002/jat.2804.

48. EMBL-EBI ChEMBL Database Available online: https://www.ebi.ac.uk/chembl/ (accessed on Oct 1, 2021).

49. ChEMBL Kappa opioid receptor Target Report Card Available online: https://www.ebi.ac.uk/chembl/target_report_card/CHEMBL237/ (accessed on Oct 13, 2021).

50. ChEMBL Delta opioid receptor Target Report Card Available online: https://www.ebi.ac.uk/chembl/target_report_card/CHEMBL236/ (accessed on Oct 18, 2021).

51. ChEMBL Mu opioid receptor Target Report Card Available online: https://www.ebi.ac.uk/chembl/target_report_card/CHEMBL233/ (accessed on Oct 13, 2021).

52. Chemical Computing Group ULC Molecular Operating Enviroment (MOE), 2020.0901 2021.

53. Gerber, P.; Müller, K. MAB, a generally applicable molecular force field for structure modelling in medicinal chemistry. *J. Comput. Aided. Mol. Des.* **1995**, *9*, 251–268, doi:10.1007/BF00124456.

54. RCSB PDB: Homepage Available online: https://www.rcsb.org/ (accessed on Feb 4, 2021).

55. Ellis, C.R.; Kruhlak, N.L.; Kim, M.T.; Hawkins, E.G.; Stavitskaya, L. Predicting opioid receptor binding affinity of pharmacologically unclassified designer substances using molecular docking. *PLoS One* **2018**, *13*, doi:10.1371/journal.pone.0197734.

56. Isomer Design Available online: https://isomerdesign.com (accessed on Nov 17, 2021).

57. Huang, W.; Manglik, A.; Venkatakrishnan, A.; Laeremans, T.; Feinberg, E.; Sanborn, A.; HE,

K.; KE, L.; TS, T.; RC, K.; et al. Structural insights into μ-opioid receptor activation. *Nature* **2015**, *524*, 315–321, doi:10.1038/NATURE14886.

58. RCSB PDB 5C1M: Crystal structure of active mu-opioid receptor bound to the agonist BU72 Available online: https://www.rcsb.org/structure/5C1M (accessed on Oct 12, 2021).

59. Claff, T.; Yu, J.; Blais, V.; Patel, N.; Martin, C.; Wu, L.; Han, G.W.; Holleran, B.J.; Van der Poorten, O.; White, K.L.; et al. Elucidating the active δ-opioid receptor crystal structure with peptide and small-molecule agonists. *Sci. Adv.* **2019**, *5*, eaax9115, doi:10.1126/SCIADV.AAX9115.

60. RCSB PDB 6PT3: Crystal structure of the active delta opioid receptor in complex with the small molecule agonist DPI-287 Available online: https://www.rcsb.org/structure/6PT3 (accessed on Oct 12, 2021).

61. Che, T.; Majumdar, S.; Zaidi, S.A.; Ondachi, P.; McCorvy, J.D.; Wang, S.; Mosier, P.D.; Uprety, R.; Vardy, E.; Krumm, B.E.; et al. Structure of the Nanobody-Stabilized Active State of the Kappa Opioid Receptor. *Cell* **2018**, *172*, 55-67.e15, doi:10.1016/J.CELL.2017.12.011.

62. RCSB PDB 6B73: Crystal Structure of a nanobody-stabilized active state of the kappa-opioid receptor Available online: https://www.rcsb.org/structure/6B73 (accessed on Oct 12, 2021).

63. Krumm, B.E.; Grisshammer, R. Peptide ligand recognition by G protein-coupled receptors. *Front. Pharmacol.* **2015**, *6*, 48, doi:10.3389/FPHAR.2015.00048/BIBTEX.

64. Shim, J.; Coop, A.; Mackerell, A.D. Molecular details of the activation of the μ opioid receptor. *J. Phys. Chem. B* **2013**, *117*, 7907–7917, doi:10.1021/JP404238N.

65. Vandeputte, M.M.; Van Uytfanghe, K.; Layle, N.K.; St. Germaine, D.M.; Iula, D.M.; Stove, C.P. Synthesis, Chemical Characterization, and μ-Opioid Receptor Activity Assessment of the Emerging Group of "nitazene" 2-Benzylbenzimidazole Synthetic Opioids. *ACS Chem. Neurosci.* **2021**, *12*, 1241–1251, doi:10.1021/ACSCHEMNEURO.1C00064/SUPPL_FILE/CN1C00064_SI_001.PDF.

66. Casy, A.F.; Parfitt, R.T. *Opioid analgesics : chemistry and receptors*; 1st ed.; Springer US: New York, 1986; ISBN 978-1-4899-0587-1.

67. Manglik, A. Molecular Basis of Opioid Action: From Structures to New Leads. *Biol. Psychiatry* **2020**, *87*, 6–14, doi:10.1016/J.BIOPSYCH.2019.08.028.

68. Zimmerman, D.M.; Leander, J.D. Selective opioid receptor agonists and antagonists: research tools and potential therapeutic agents. *J. Med. Chem.* **1990**, *33*, 895–902, doi:10.1021/JM00165A002.

69. Shim, J.; Coop, A.; MacKerell, J.A.D. Consensus 3D Model of μ-Opioid Receptor Ligand Efficacy Based on a Quantitative Conformationally Sampled Pharmacophore. *J. Phys. Chem. B* **2011**, *115*, 7487–7496, doi:10.1021/JP202542G.

70. Singh, N.; Nolan, T.; McCurdy, C. Chemical function-based pharmacophore development for novel, selective kappa opioid receptor agonists. *J. Mol. Graph. Model.* **2008**, *27*, 131–139, doi:10.1016/J.JMGM.2008.03.007.

71. Zhang, J.; Liu, G.; Tang, Y. Chemical function-based pharmacophore generation of selective kappa-opioid receptor agonists by catalyst and phase. *J. Mol. Model.* **2009**, *15*, 1027–1041, doi:10.1007/S00894-008-0418-5.

72. Tricklebank, M.D.; Honore, T.; Iversen, S.D.; Kemp, J.A.; Knight, A.R.; Marshall, G.R.; Rupniak, N.M.J.; Singh, L.; Tye, S.; Watjen, F.; et al. The pharmacological properties of the imidazobenzodiazepine, FG 8205, a novel partial agonist at the benzodiazepine receptor. *Br. J. Pharmacol.* **1990**, *101*, 753–761, doi:10.1111/J.1476-5381.1990.TB14152.X.

73. Krall, J.; Balle, T.; Krogsgaard-Larsen, N.; Sørensen, T.E.; Krogsgaard-Larsen, P.; Kristiansen, U.; Frølund, B. GABAA receptor partial agonists and antagonists: structure, binding mode, and pharmacology. *Adv. Pharmacol.* **2015**, *72*, 201–227, doi:10.1016/BS.APHA.2014.10.003.

74. Zhou, S.; Zhang, S.; Wang, L.; Huang, S.; Yuan, Y.; Yang, J.; Wang, H.; Li, X.; Wang, P.; Zhou, L.; et al. BET protein inhibitor JQ1 downregulates chromatin accessibility and suppresses metastasis of gastric cancer via inactivating RUNX2/NID1 signaling. *Oncog. 2020 93* **2020**, *9*, 1–14, doi:10.1038/s41389-020-0218-z.

75. Prost-Marechal, J. Imidazobenzodiazepines and their salt 1982.

76. Weber, K.H.; Kuhn, F.J.; Böke-Kuhn, K.; Lehr, E.; Danneberg, P.B.; Hommer, D.; Paul, S.M.; Skolnick, P. Pharmacological and neurochemical properties of 1,4-diazepines with two annelated heterocycles ('hetrazepines'). *Eur. J. Pharmacol.* **1985**, *109*, 19–31, doi:10.1016/0014-2999(85)90535-7.

77. Godel, T.; Hunkeler, W.; Stadler, H.; Widmer, U. US5665718A Imidazodiazepines 1997.

78. van Gerven, J.; Roncari, G.; Schoemaker, R.; Massarella, J.; Keesmaat, P.; Kooyman, H.; Heizmann, P.; Zell, M.; Cohen, A.; Dingemanse, J. Integrated pharmacokinetics and pharmacodynamics of Ro 48-8684, a new benzodiazepine, in comparison with midazolam during first administration to healthy male subjects. *Br. J. Clin. Pharmacol.* **1997**, *44*, 487–493, doi:10.1046/J.1365-2125.1997.T01-1-00613.X.

79. Hering, W.; Ihmsen, H.; Albrecht, S.; Schwilden, H.; Schüttler, J. [RO 48-6791--a short acting benzodiazepine. Pharmacokinetics and pharmacodynamics in young and old subjects in comparison to midazolam]. *Anaesthesist* **1996**, *45*, 1211–1214, doi:10.1007/S001010050360.

80. Wrigley, P.J.; Elliott, D.W.; Blake, D. A Phase 2 Clinical Trial Comparing Ro 48–6791, a New Short-Acting Benzodiazepine, with Propofol for Induction of Anaesthesia: *https://doi.org/10.1177/0310057X9802600506* **2019**, *26*, 509–514, doi:10.1177/0310057X9802600506.

81. Miller, R.; Gropper, M. *Miller's Anesthesia*; Gropper, M., Eriksson, L., Fleisher, L., Wiener-Kronish, J., Cohen, N., Leslie, K., Eds.; 9th ed.; 2019; Vol. I–II; ISBN 9780323596046.

82. Ramírez, D.; Caballero, J. Is It Reliable to Take the Molecular Docking Top Scoring Position as the Best Solution without Considering Available Structural Data? *Molecules* **2018**, *23*, doi:10.3390/MOLECULES23051038.

83. Jakhar, R.; Dangi, M.; Khichi, A.; Chhillar, A.K. Relevance of Molecular Docking Studies in Drug Designing. *Curr. Bioinform.* **2019**, *15*, 270–278, doi:10.2174/1574893615666191219094216.

84. Manglik, A.; Kruse, A.C.; Kobilka, T.S.; Thian, F.S.; Mathiesen, J.M.; Sunahara, R.K.; Pardo, L.; Weis, W.I.; Kobilka, B.K.; Granier, S. Crystal structure of the μ-opioid receptor bound to a morphinan antagonist. *Nat. 2012 4857398* **2012**, *485*, 321–326, doi:10.1038/nature10954.

85. McKernan, R.M.; Rosahl, T.W.; Reynolds, D.S.; Sur, C.; Wafford, K.A.; Atack, J.R.; Farrar, S.; Myers, J.; Cook, G.; Ferris, P.; et al. Sedative but not anxiolytic properties of benzodiazepines are mediated by the GABAA receptor α1 subtype. *Nat. Neurosci. 2000 36* **2000**, *3*, 587–592, doi:10.1038/75761.

86. Dripps, I.J.; Jutkiewicz, E.M. Delta Opioid Receptors and Modulation of Mood and Emotion. In *Handbook of Experimental Pharmacology*; Springer, Cham, 2017; Vol. 247, pp. 179–197.

87. Gendron, L.; Cahill, C.M.; Zastrow, M. von; Schiller, P.W.; Pineyro, G. Molecular Pharmacology of δ-Opioid Receptors. *Pharmacol. Rev.* **2016**, *68*, 631,

doi:10.1124/PR.114.008979.

88. Jutkiewicz, E. The antidepressant -like effects of delta-opioid receptor agonists. *Mol. Interv.* **2006**, *6*, 162–169, doi:10.1124/MI.6.3.7.

89. Rudolph, U.; Crestani, F.; Benke, D.; Brünig, I.; Benson, J.A.; Fritschy, J.M.; Martin, J.R.; Bluethmann, H.; Möhler, H. Benzodiazepine actions mediated by specific γ-aminobutyric acid(A) receptor subtypes. *Nature* **1999**, *401*, 796–800, doi:10.1038/44579.

90. Reddy, S.; Patt, R.B. The benzodiazepines as adjuvant analgesics. *J. Pain Symptom Manage.* **1994**, *9*, 510–514, doi:10.1016/0885-3924(94)90112-0.

91. Inoue, A.; Ishiguro, J.; Kitamura, H.; Arima, N.; Okutani, M.; Shuto, A.; Higashiyama, S.; Ohwada, T.; Arai, H.; Makide, K.; et al. TGFα shedding assay: an accurate and versatile method for detecting GPCR activation. *Nat. Methods 2012 910* **2012**, *9*, 1021–1029, doi:10.1038/nmeth.2172.

Table 1 Binding values (S) generated for the ten molecules that showed the highest predicted values of log1/c, docked within the 6HUP and 6HUO receptors.

Notes: The molecules are listed in decreasing order, within each OR type, of their predicted log1/c (biological activity); alprazolam and diazepam are prescription medications and here included only as a reference, because they are the respective bound ligand of 6HUO and 6HUP.

MOR	
Molecule	SMILESs
BU72	O(C)[C@]12[C@]3(C)[C@@H](c4ccccc4)[NH2+][C@H]1[C@@]14c5c(ccc(O)c5)C[C@@H]([NH+](C)CC1 C3
Ro 48-6791	Fc1cc2C(=O)N(C)Cc3c(-c4nc(CN(CCC)CCC)on4)ncn3-c2cc1
Ro 48-8684	Fc1cc2C(=O)N(C)Cc3c(-c4oc(C[NH+](CCC)CCC)cn4)ncn3-c2cc1
Fluloprazolam	Fc1c(C2=NCC=3N(C(=O)C(=CN4CC[NH+](C)CC4)N=3)c3c2cc([N+](=O)[O-])cc3)cccc1
Ciclotizolam	Brc1sc2-n3c(C4CCCCC4)nnc3C[NH+]=C(c3c(Cl)cccc3)c2c1
Ro 15-9270	Clc1c(C=2c3c(-n4c(C)nnc4CC=2)ccc([N+](=O)[O-])c3)cccc1
Pynazolam	O=[N+]([O-])c1cc2C(c3ncccc3)=NCc3n(c(C)nn3)-c2cc1
Tuclazepam	Clc1c(C2=[NH+]CC(CO)N(C)c3c2cc(Cl)cc3)cccc1
Deschloroetizolam	C(C)c1sc2-n3c(C)nnc3C[NH+]=C(c3ccccc3)c2c1
Metizolam	Clc1c(C2=[NH+]Cc3n(-c4sc(CC)cc24)cnn3)cccc1
KOR	
MP11 04	C1CC1CN2CC[C@]34[C@@H]5[C@H]2CC6=C3C(=C(C=C6)O)O[C@H]4[C@@H](C=C5)NC(=O)C7=CC
Fluloprazolam	Fc1c(C2=NCC=3N(C(=O)C(=CN4CC[NH+](C)CC4)N=3)c3c2cc([N+](=O)[O-])cc3)cccc1
Ro 48-6791	Fc1cc2C(=O)N(C)Cc3c(-c4nc(CN(CCC)CCC)on4)ncn3-c2cc1
Ciclotizolam	Brc1sc2-n3c(C4CCCCC4)nnc3C[NH+]=C(c3c(Cl)cccc3)c2c1
Cinazepam	Brc1cc2C(c3c(Cl)cccc3)=NC(OC(=O)CCC(=O)[O-])C(=O)Nc2cc1
JQ1	Clc1ccc(C2=[NH+]C(CC(=O)OC(C)(C)C)c3n(c(C)nn3)-c3sc(C)c(C)c23)cc1
Devazepide	O=C(N[C@@H]1C(=O)N(C)c2c(C(c3ccccc3)=N1)cccc2)c1[nH]c2c(c1)cccc2
Ro 48-8684	Fc1cc2C(=O)N(C)Cc3c(-c4oc(C[NH+](CCC)CCC)cn4)ncn3-c2cc1
Arfendazam	Clc1cc2N(c3ccccc3)C(=O)CCN(C(=O)OCC)c2cc1
Ro 17-1812	Clc1c2C(=O)N3C(c4c(C(=O)OCC5CC5)ncn4-c2ccc1)CC3
DOR	
DPI-287	O=C(N(CC)CC)c1ccc([C@@H](N2[C@@H](C)C[NH+](CC=C)[C@H](C)C2)c2cc(O)ccc2)cc1
Ro 48-8684	Fc1cc2C(=O)N(C)Cc3c(-c4oc(C[NH+](CCC)CCC)cn4)ncn3-c2cc1
JQ1	Clc1ccc(C2=[NH+][C@H](CC(=O)OC(C)(C)C)c3n(c(C)nn3)-c3sc(C)c(C)c23)cc1
Fluloprazolam	Fc1c(C2=NCC=3N(C(=O)/C(=C/N4CC[NH+](C)CC4)/N=3)c3c2cc([N+](=O)[O-])cc3)cccc1
Ciclotizolam	Brc1sc2-n3c(C4CCCCC4)nnc3C[NH+]=C(c3c(Cl)cccc3)c2c1
Ro 48-6791	Fc1cc2C(=O)N(C)Cc3c(-c4nc(CN(CCC)CCC)on4)ncn3-c2cc1
Elfazepam	Clc1cc2C(c3c(F)cccc3)=NCC(=O)N(CCS(=O)(=O)CC)c2cc1
Metaclazepam	Brc1cc2C(c3c(Cl)cccc3)=[NH+]C[C@H](COC)N(C)c2cc1
Ethyl Carfluzepate	Clc1cc2C(c3c(F)cccc3)=N[C@H](C(=O)OCC)C(=O)N(C(=O)NC)c2cc1
Fluadinazolam	Clc1cc2C(c3c(F)cccc3)=NCc3n(c(C[NH+](C)C)nn3)-c2cc1
Devazepide	O=C(N[C@@H]1C(=O)N(C)c2c(C(c3ccccc3)=N1)cccc2)c1[nH]c2c(c1)cccc2

Table 2 Most common interactions identified between the DBDZs ligands and the ORs

Receptor	**Residue**	**Interaction**
MOR	Asp 147	side chain H-donor/ionic

	Met 151	sidechain H-donor
	Val300	Arene-H interaction
	His297	hydrogen bonds water mediated.
	Lys233	hydrogen bonds water mediated.
DOR	Asp 128	sidechain H-donor/ionic
	Met 132	sidechain H-donor
	Val 281	Arene-H interaction
	His 278	H-Arene interaction
KOR	Asp 138	sidechain H-donor
	Met 142	sidechain H-donor
	Ser 211	side chain hydrogen acceptor
	Leu 212	hydrogen acceptor
	Glu 115	Backbone hydrogen acceptor
	Tyr139	Arene-Arene interaction
	Ile 316	Backbone hydrogen acceptor.

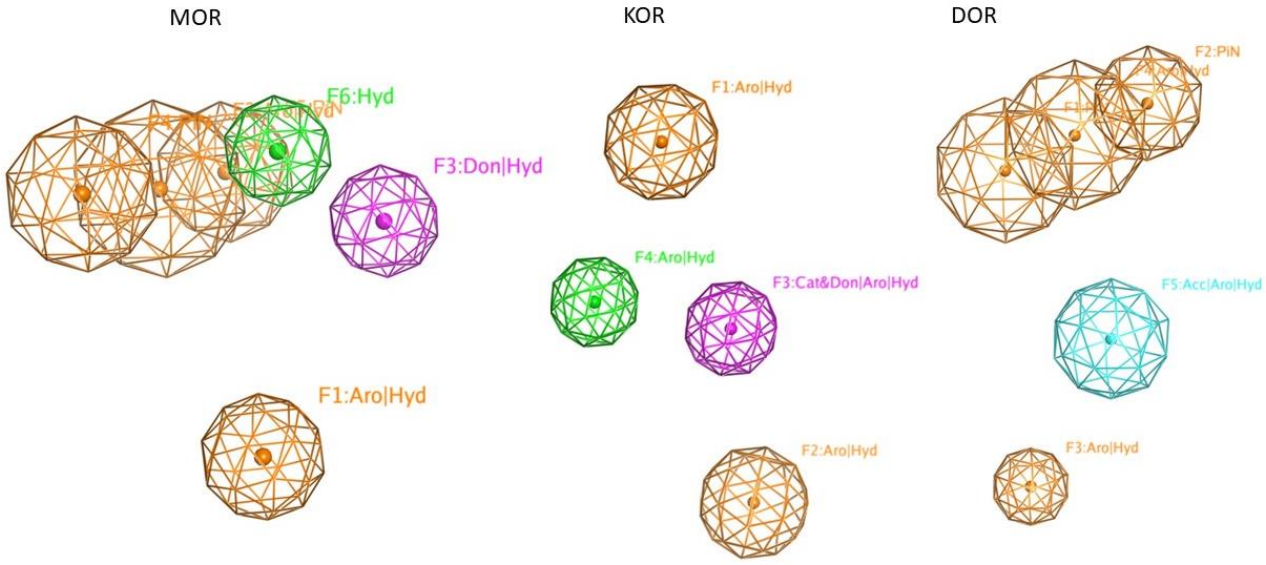

Figure 1.Pharmacophore queries generated for MOR, KOR and DOR.

Notes: On the left side, the pharmacophore query obtained from the flexible alignment of the 20 strong agonist binders for MOR, in the middle for KOR and on the right side for DOR. It can be seen from the pictures that different spatial coordinates may host more than one feature. In orange are represented the aromatic/hydrophobic centroids, in green the hydrophobic centroid only, in purple the H-bond donor/ hydrophobic centroid for MOR with the addiction of the cationic atom, and in light blue the H-bond acceptor, aromatic/hydrophobic centroid.

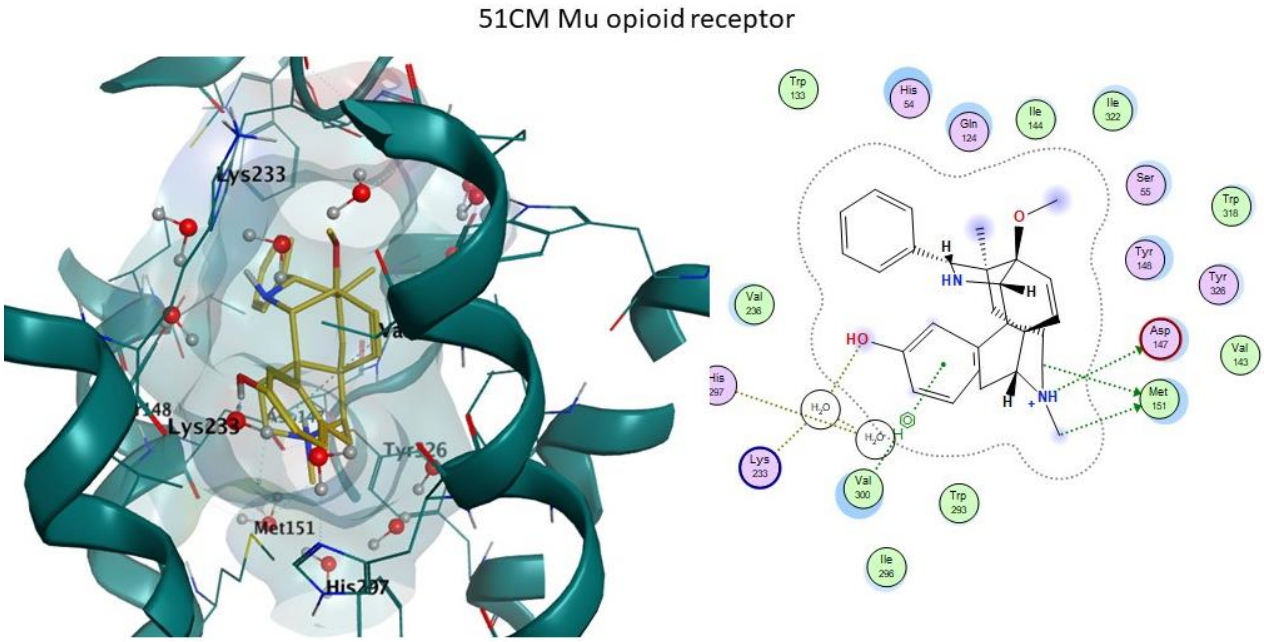

Figure 2 5C1M mu opioid receptor (RCSB PDB, 2015) binding site 3D and 2D representations.

Notes: 5C1M binding site; on the left, the binding pocket 3D representation. The green portion represents the receptor backbone and the side chains of the amino acid residues forming the binding pocket whilst the gold one is the co-crystallised ligand BU72. On the right side, a 2D representation of the binding pocket and interactions between receptor residues and ligand is provided.

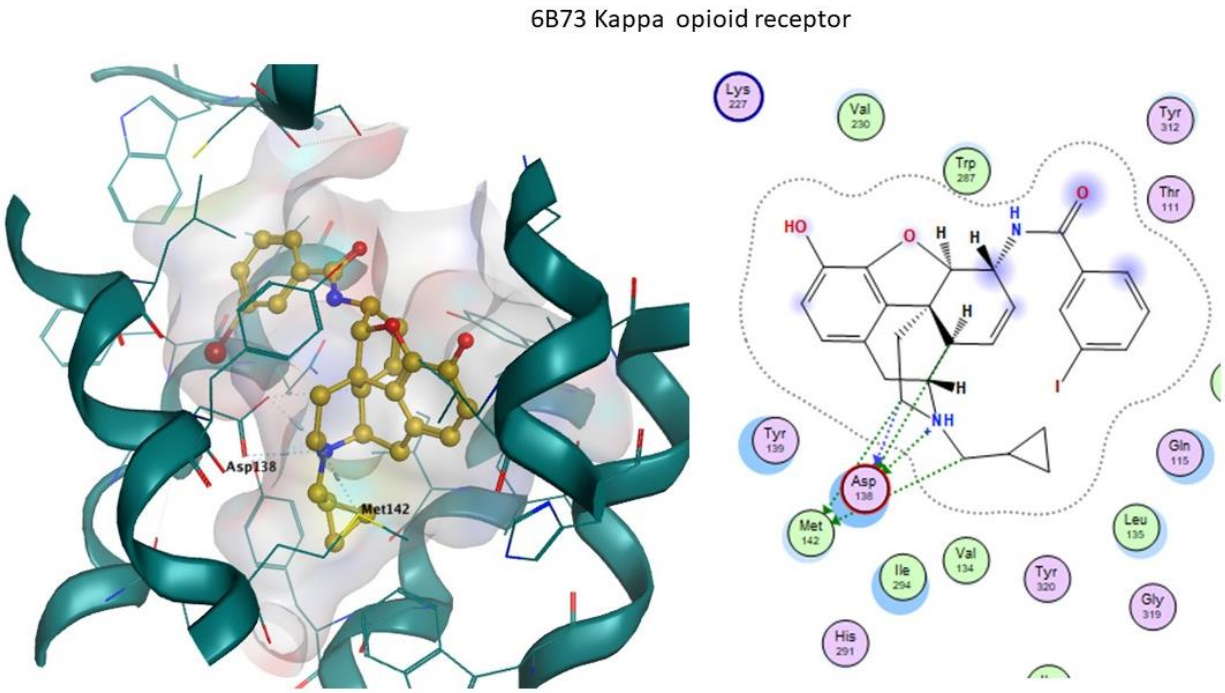

Figure 36B73 kappa opioid receptor (RCSB PDB, 2018) binding site 3D and 2D representations.

Notes: 6B73 binding site; on the left, the binding pocket 3D representation. The green portion represents the receptor backbone and the side-chains of the amino acids residues forming the binding pocket whilst the gold one is the co-crystallised ligand MP11 04. The see-through cloud in the binding pocket represents the pocket surface. On the right side, the 2D representation of the binding pocket and the interactions between receptor residues and ligand are provided.

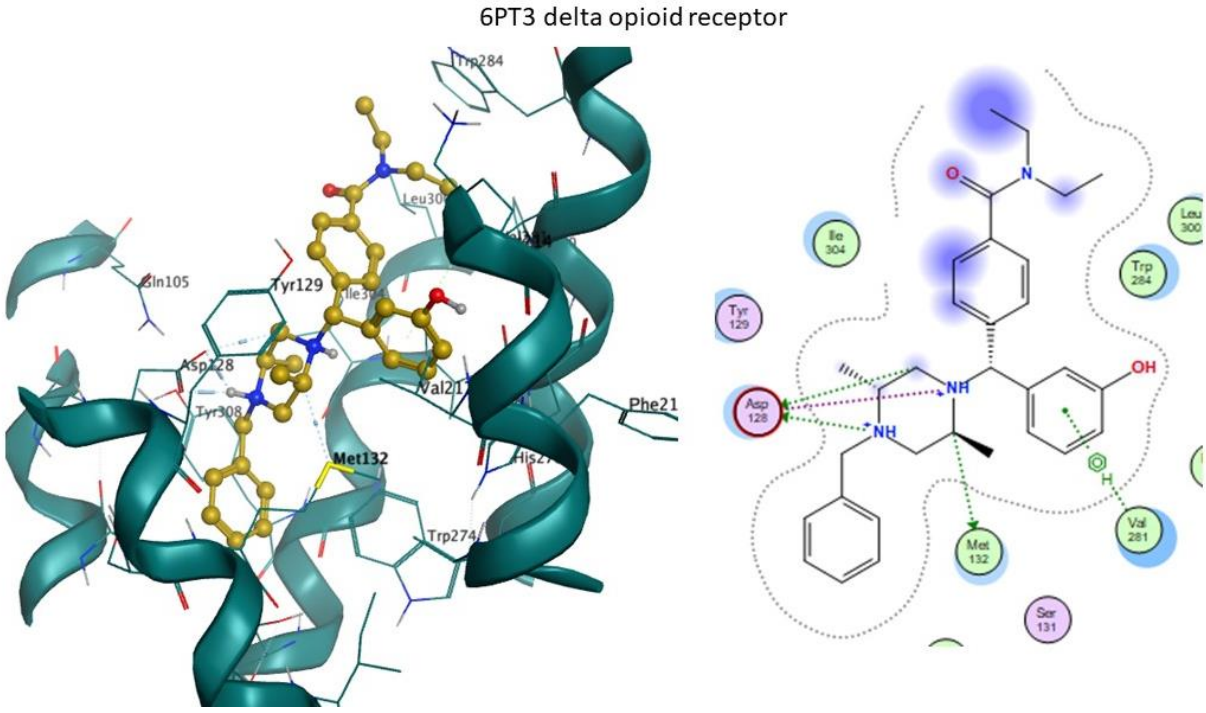

Figure 4 6PT3 delta opioid receptor (RCSB PDB, 2018) binding site 3D and 2D representations.

Notes: 6PT3 binding site; on the left, the binding pocket 3D representation. The green portion represents the receptor backbone and the side-chains of the amino acids residues forming the binding pocket whilst the gold one is the co-crystallised ligand DPI-287. On the right side, the 2D representation of the binding pocket and the interactions between receptor residues and ligand is provided

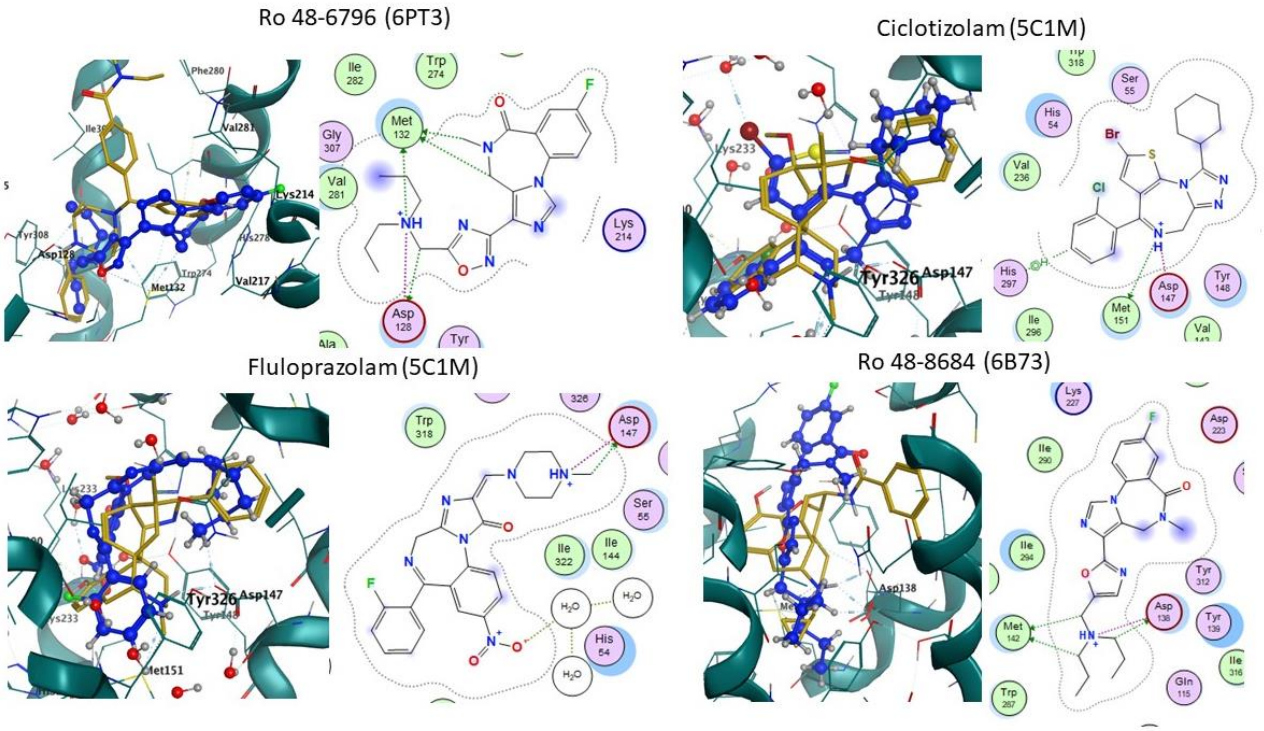

Figure 5 3D and 2D interactions for fluloprazolam, ciclotizolam, Ro 48-8684 and Ro 48-6796

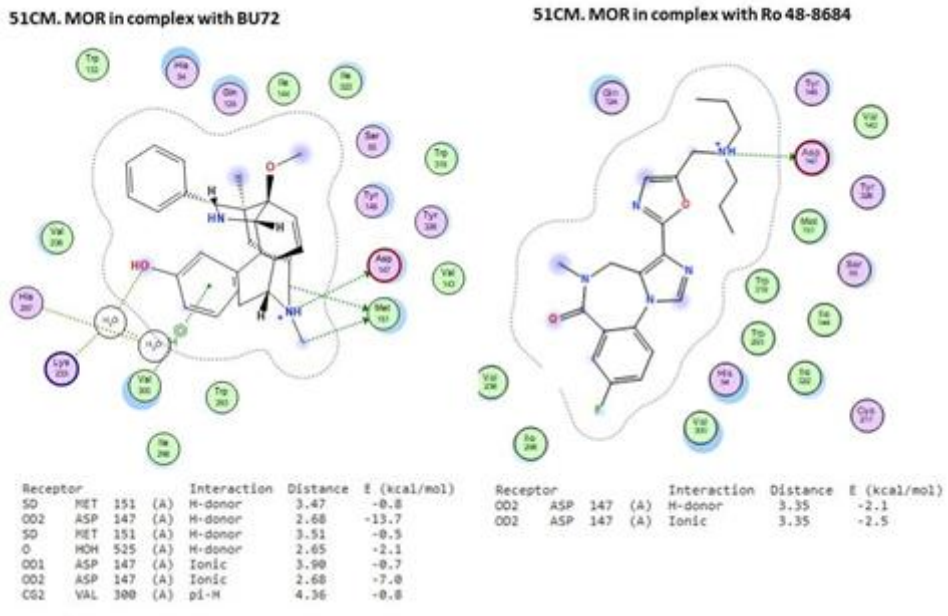

Figure 6 2D representation of the interactions between BU72, Ro 48-8684 and the binding pocket of MOR. In the tables, the amino acid residues involved in the interaction are reported, together with the type of interactions, their length (expressed in Angstrom, Å) and their energy (expressed in Kcal/mol)

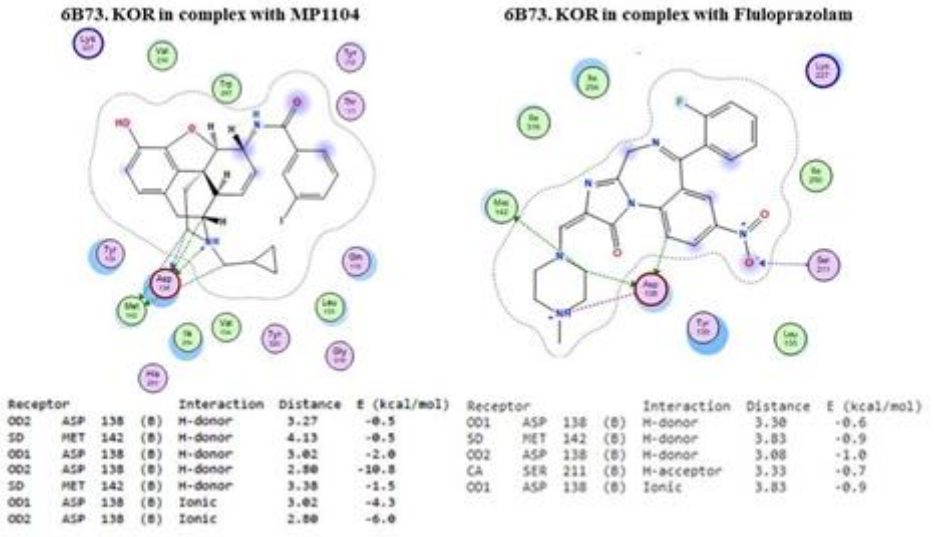

Receptor				Interaction	Distance	E (kcal/mol)
OD2	ASP	138	(B)	H-donor	3.27	-0.5
SD	MET	142	(B)	H-donor	4.13	-0.5
OD1	ASP	138	(B)	H-donor	3.02	-2.0
OD2	ASP	138	(B)	H-donor	2.80	-10.8
SD	MET	142	(B)	H-donor	3.38	-1.5
OD1	ASP	138	(B)	Ionic	3.02	-4.3
OD2	ASP	138	(B)	Ionic	2.80	-6.0

Receptor				Interaction	Distance	E (kcal/mol)
OD1	ASP	138	(B)	H-donor	3.30	-0.6
SD	MET	142	(B)	H-donor	3.83	-0.9
OD2	ASP	138	(B)	H-donor	3.08	-1.0
CA	SER	211	(B)	H-acceptor	3.33	-0.7
OD1	ASP	138	(B)	Ionic	3.83	-0.9

Figure 7 2D representation of the interactions between MP11-04, fluloprazolam and the binding pocket of KOR. In the tables, the amino acid residues involved in the interaction are reported, together with the type of interactions, their length (expressed in Angstrom, Å) and their energy (expressed in Kcal/mol)

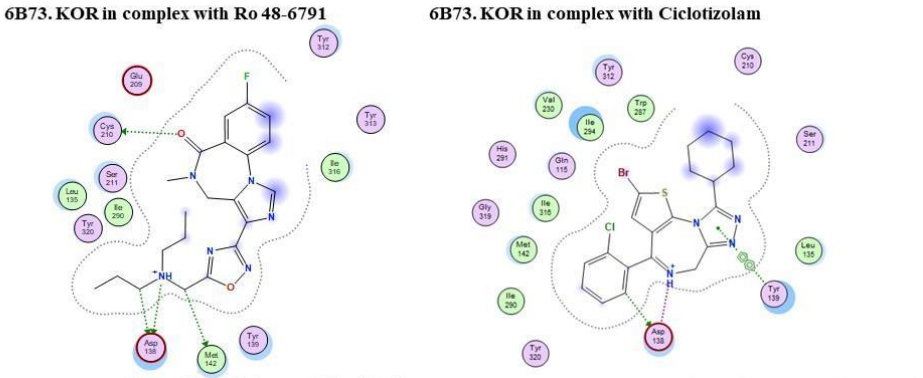

Receptor				Interaction	Distance	E (kcal/mol)
SG	CYS	210	(B)	H-donor	3.44	-0.5
OD2	ASP	138	(B)	H-donor	2.74	-11.8
SD	MET	142	(B)	H-donor	3.64	-1.1
OD1	ASP	138	(B)	H-donor	2.99	-2.2
OE1	GLU	209	(B)	H-donor	3.11	-0.7
OD1	ASP	138	(B)	Ionic	3.23	-3.1
OD2	ASP	138	(B)	Ionic	2.74	-6.4

Receptor				Interaction	Distance	E (kcal/mol)
OD2	ASP	138	(B)	H-donor	3.23	-0.8
OD1	ASP	138	(B)	Ionic	3.74	-1.1
OD2	ASP	138	(B)	Ionic	3.13	-3.7
6-ring	TYR	139	(B)	pi-pi	3.52	-0.0

Figure 8 2D representation of the interactions between Ro 48-679, ciclotizolam and the binding pocket of KOR. In the tables, the amino acid residues involved in the interaction are reported, together with the type of interactions, their length (expressed in Angstrom, Å) and their energy (expressed in Kcal/mol).

6PT3. DOR in complex with DPI-287

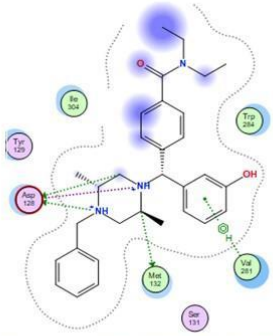

Receptor				Interaction	Distance	E (kcal/mol)
SD	MET	132	(A)	H-donor	3.34	-0.7
OD2	ASP	128	(A)	H-donor	2.97	-2.0
OD1	ASP	128	(A)	H-donor	2.72	-10.9
OD2	ASP	128	(A)	H-donor	2.92	-6.1
OD2	ASP	128	(A)	Ionic	3.87	-0.8
OD1	ASP	128	(A)	Ionic	2.72	-6.7
OD2	ASP	128	(A)	Ionic	2.92	-5.0
CG1	VAL	281	(A)	pi-H	3.94	-0.6

6PT3. DOR in complex with Fluloprazolam

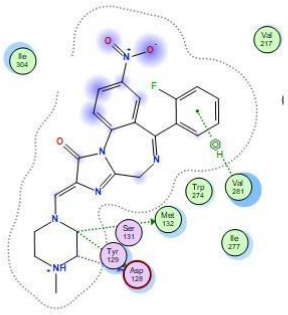

Receptor				Interaction	Distance	E (kcal/mol)
OD1	ASP	128	(A)	H-donor	3.21	-0.9
SD	MET	132	(A)	H-donor	4.50	-0.5
O	ASP	128	(A)	H-donor	3.32	-0.5
CG1	VAL	281	(A)	pi-H	3.81	-0.7

6PT3. DOR in complex with Ro 48-8684

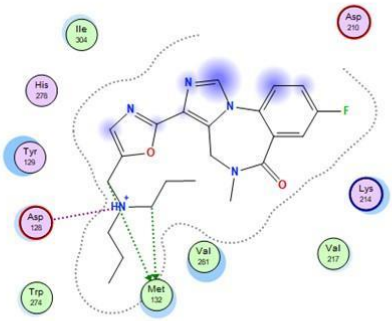

Receptor				Interaction	Distance	E (kcal/mol)
SD	MET	132	(A)	H-donor	4.33	-0.9
SD	MET	132	(A)	H-donor	3.65	-0.5
OD1	ASP	128	(A)	Ionic	3.20	-3.3
OD2	ASP	128	(A)	Ionic	3.56	-1.7

Figure 9 2D representation of the interactions between DPI-287 (co-crystallised ligand), fluloprazolam, Ro 48-8684 and the binding pocket of DOR. In the tables, the amino acid residues involved in the interaction are reported, together with the type of interactions, their length (expressed in Angstrom, Å) and their energy (expressed in Kcal/mol).